Supplementary Figure 1

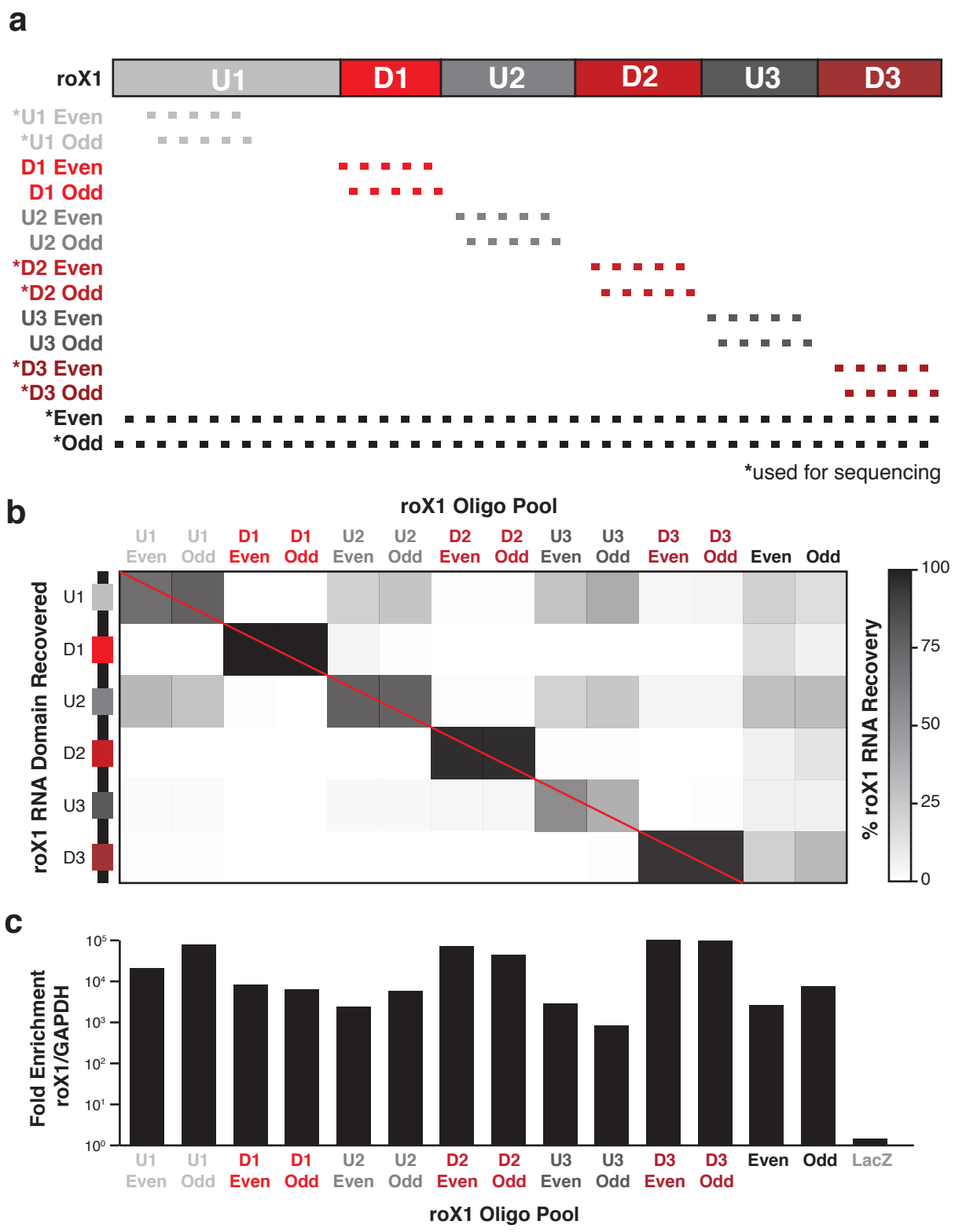

**Supplementary Figure 1**

Even-odd OPs reproduce U domain co-recovery by roX1 dChIRP.

(**a**) Schematic of roX1 dChIRP-seq oligo pool (OP) design strategy. Even and odd OPs were designed against roX1's domains. Each even-odd OP pair contains non-overlapping oligos that tile the target domain. Note that DNA fractions from U1 Even, U1 Odd, D2 Even, D2 Odd, D3 Even, D3 Odd, Even, and Odd were used for ChIRP-sequencing experiments (see **Fig. 4**).

(**b**) Analysis of RNA fragment recovery by roX1 dChIRP. RNA fragment recovery was measured by RT-qPCR, absolutely quantified against input RNA, and normalized to total roX1 RNA recovery. roX1 dChIRP efficiently recovered the targeted RNA domain (along the red diagonal). The co-recovery of U domains is reproducible across even-odd OP pairs, indicating that U domain co-recovery is not an artifact of oligo cross-hybridization.

(**c**) roX1 dChIRP specifically enriches for roX1 RNA. roX1 RNA is >1,000-fold enriched over the abundant GAPDH mRNA in roX1 dChIRP samples. LacZ does not enrich for roX1 over GAPDH.

Supplementary Figure 2

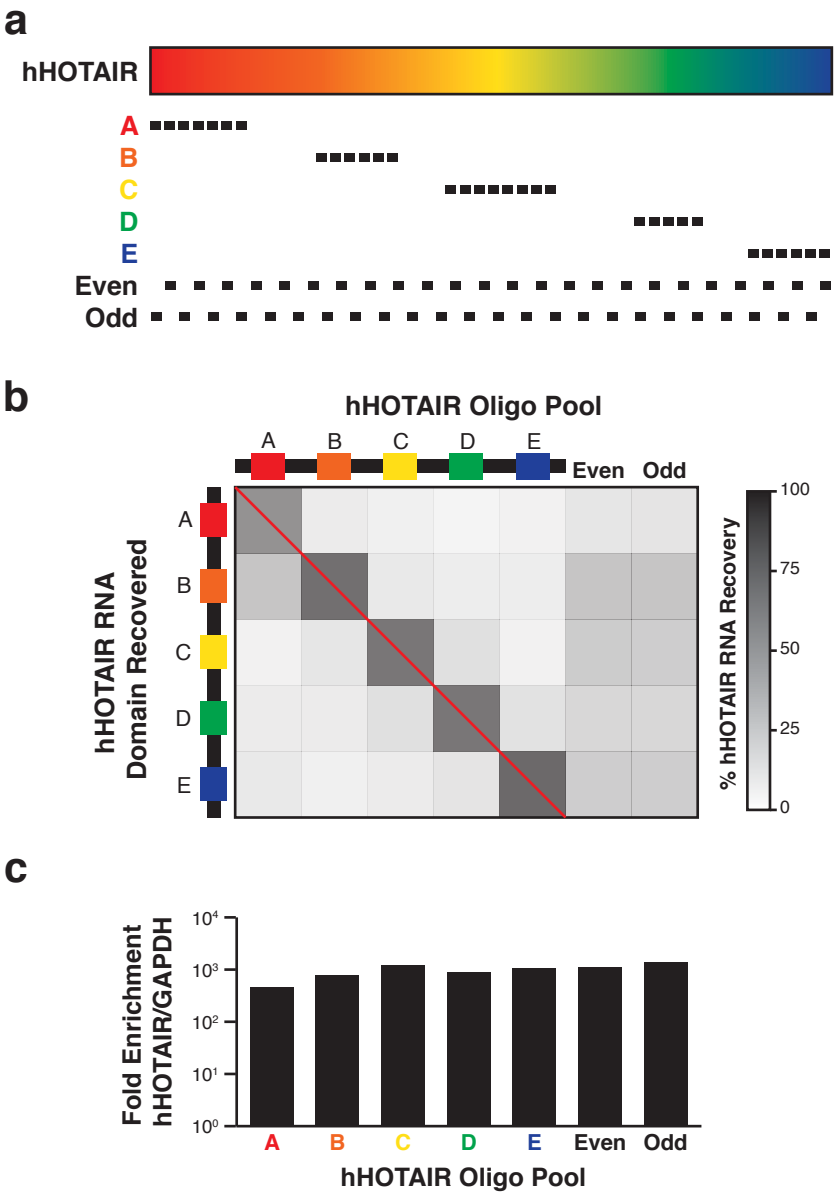

**Supplementary Figure 2**

Human HOTAIR (hHOTAIR) RNA domains are independently recovered by dChIRP.

(**a**) hHOTAIR dChIRP oligo pool design strategy. OPs were designed against five distinct regions of hHOTAIR (domains A-E), as well as Even and Odd OPs that tile the entire length of hHOTAIR.

(**b**) Analysis of RNA fragment recovery by hHOTAIR dChIRP. RNA fragment recovery was measured by RT-qPCR, absolutely quantified against input RNA, and normalized to total hHOTAIR RNA recovery. hHOTAIR dChIRP efficiently and specifically recovered the targeted RNA domain (along the red diagonal).

(**c**) hHOTAIR dChIRP specifically enriches for hHOTAIR RNA. hHOTAIR RNA is ~1,000-fold enriched over the abundant GAPDH mRNA.

Supplementary Figure 3

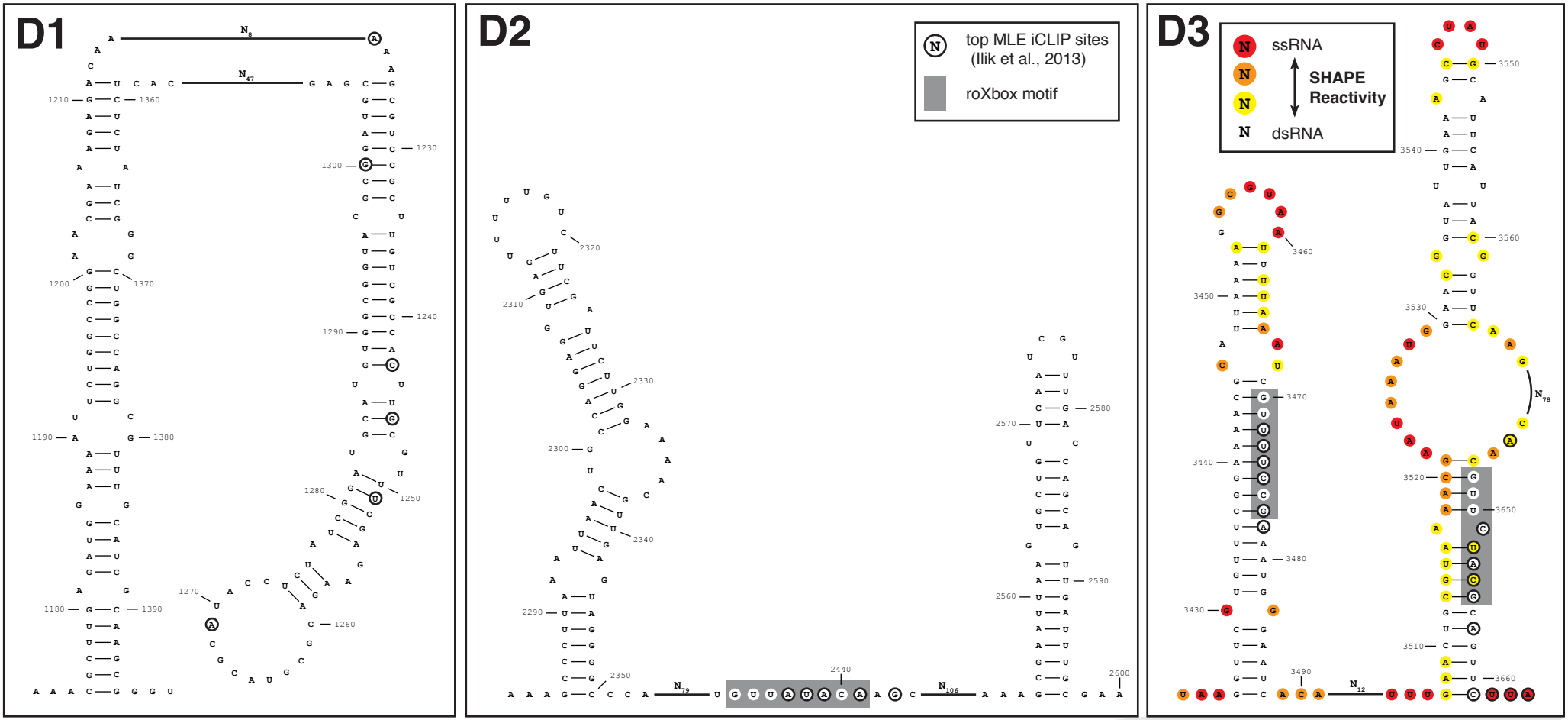


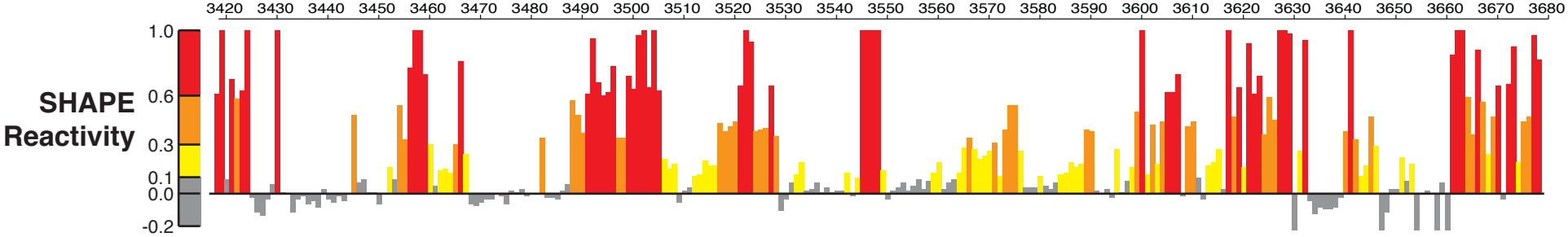

**Supplementary Figure 3**

roX1 D domains are predicted to fold into extensive linear stem-loops. Secondary structures for each roX1 domain were predicted by MFold. The D domains each contain at least two long, linear stem-loops. These structures contain the conserved roXbox motif (gray boxes) and include residues known to contact MLE protein (red circles). The structures of the D3 have previously been validated by SHAPE (selective 2'-hydroxyl acylation analyzed by primer extension), a biochemical secondary structure analysis technique[18]. Bases with high SHAPE reactivity (red, orange) are more likely to be single-stranded, whereas bases with low SHAPE reactivity (yellow, gray) are more likely to be double-stranded. The inset shows the SHAPE reactivity profile for D3, mapped onto the secondary structure model.

Supplementary Figure 4

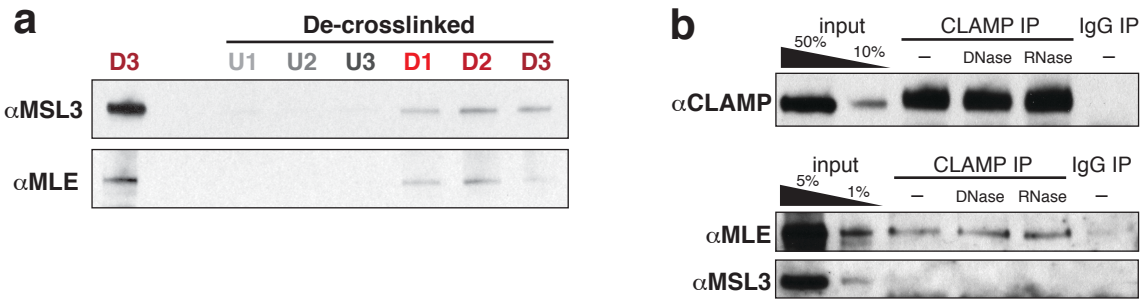

**Supplementary Figure 4**

Protein co-recovery by dChIRP and CLAMP IP.

(**a**) Thermal de-cross-linking reduces protein co-recovery by dChIRP. dChIRP was performed in cross-linked (D3; see Fig.3) or thermally de-cross-linked chromatin (de-cross-linked U1-D3). Western blotting shows that MSL3 and MLE co-recovery is greatly diminished after de-cross-linking.

(**b**) CLAMP associates with MLE in a nucleic acid-independent manner. CLAMP protein was immunoprecipitated in untreated (–), DNase-treated, and RNase-treated chromatin, and the co-recovered protein fraction was analyzed by Western blot. MLE is recovered regardless of nuclease treatment. IgG IP does not retrieve CLAMP protein.

Supplementary Figure 5

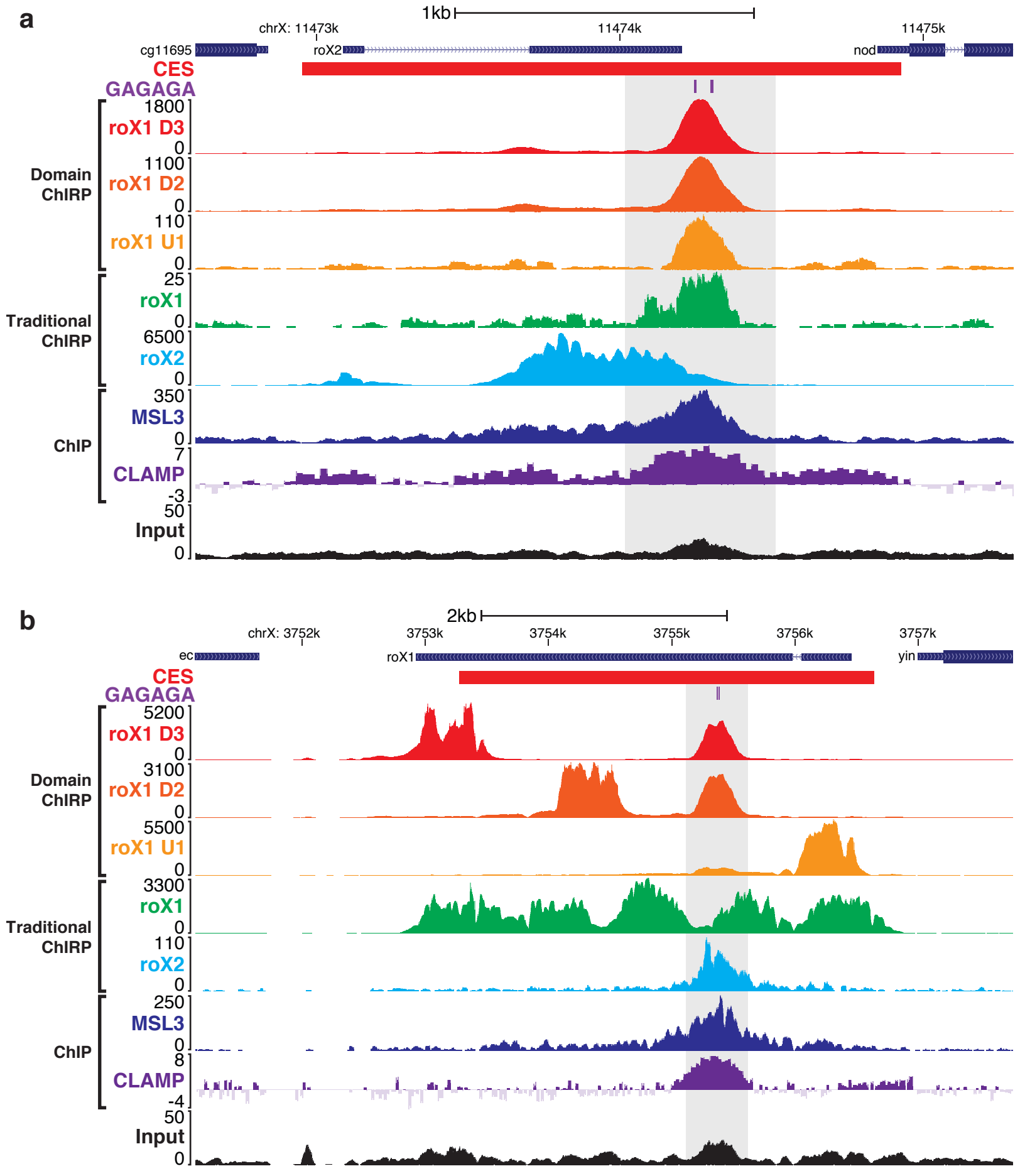

**Supplementary Figure 5**

roX1 and roX2 RNAs co-occupy both *roX* gene loci.

(**a**) roX1 occupies the *roX2* gene locus. roX1 dChIRP shows that roX1 occupies the *roX2* locus. The roX1 binding site corresponds to peaks in MSL3 and CLAMP ChIP, and contains the MRE GA-dinucleotide repeat motif. Direct oligo-DNA hybridization from roX2 ChIRP oligos obscures true RNA-dependent signal, making it impossible to resolve where roX2 RNA localizes on its own locus.

(**b**) roX1 and roX2 occupy the *roX1* locus. Traditional roX1 ChIRP produces signal along the entire roX1 gene, due to direct oligo-DNA hybridization, thus obscuring the true site of roX1-chromatin interaction. roX1 dChIRP, however, shifts this RNA-independent signal and resolves the true roX1 binding site on its own locus. This site is co-occupied by roX2, MSL3, and CLAMP, and contains the GAGA motif.

Supplementary Figure 6

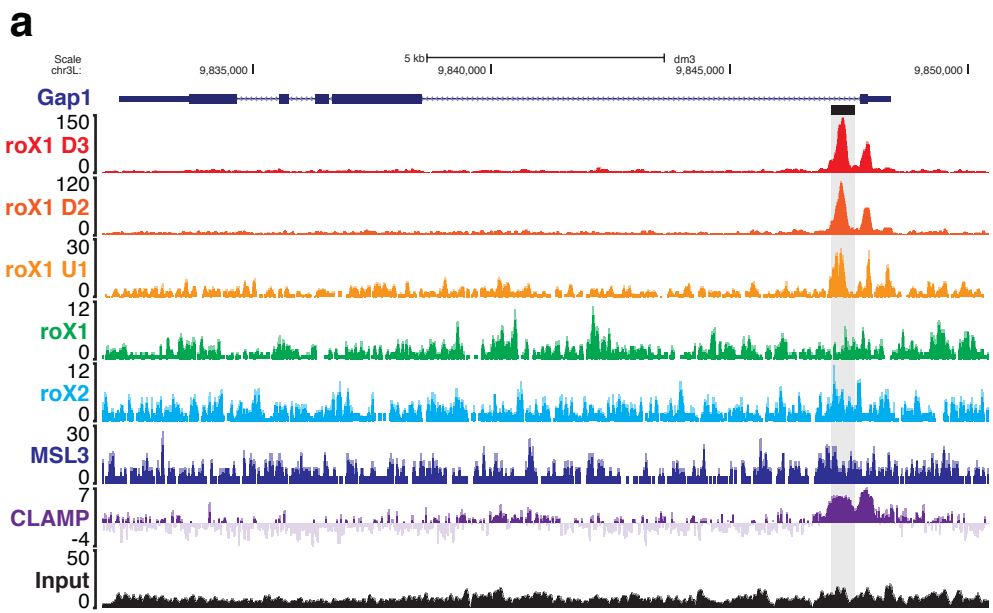


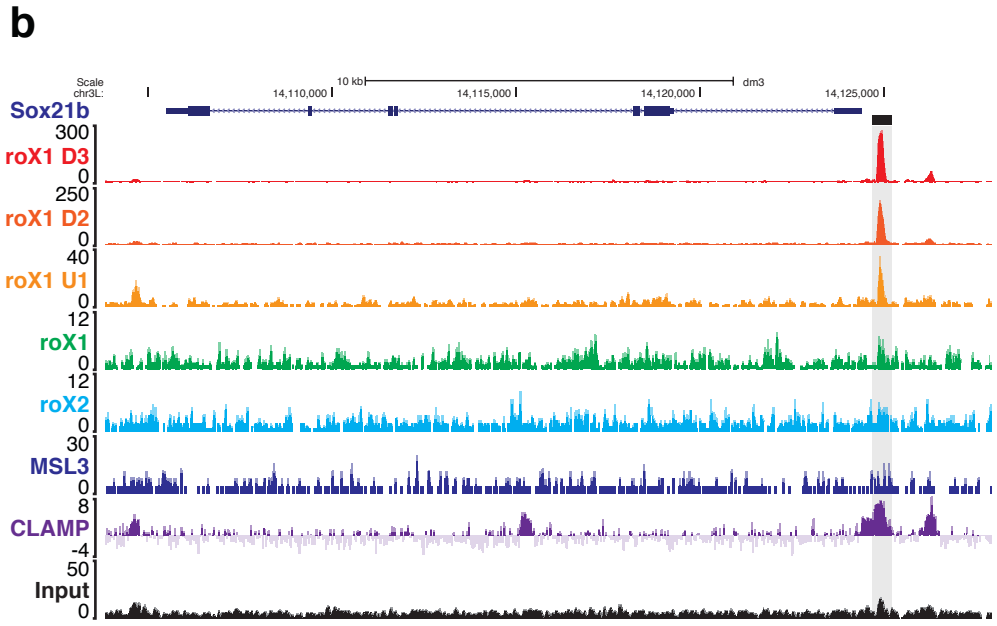


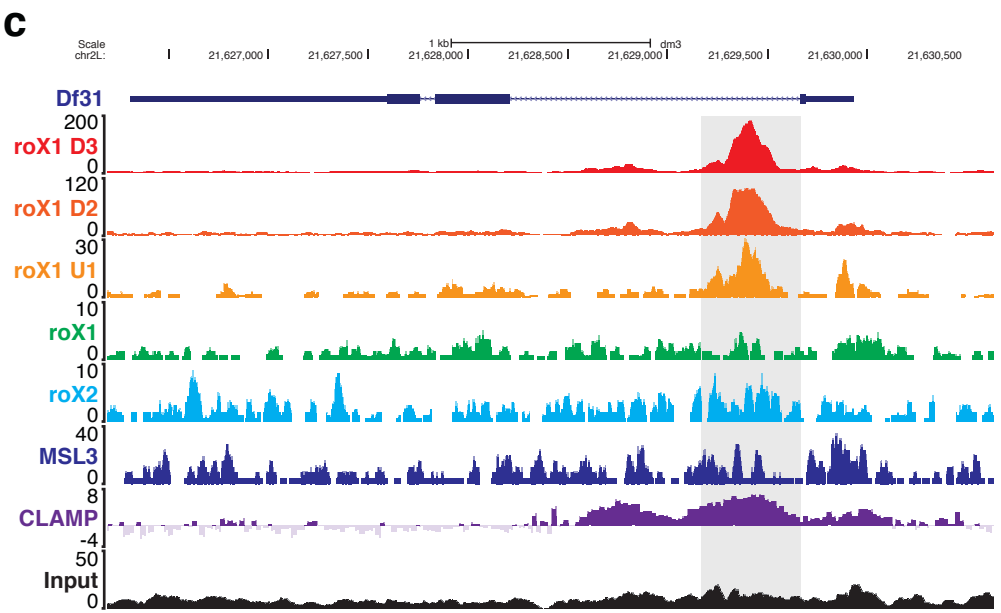


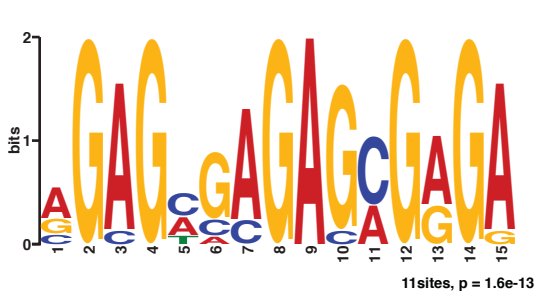

**Supplementary Figure 6**

roX1 RNA occupies several autosomal sites.

(**a-c**) roX1 dChIRP identified eleven autosomal roX1 binding sites. Sites are co-occupied by CLAMP and occur primarily (eight of the eleven) near the transcriptional start site of target genes. (**d**) The binding sites contain the MRE GA-dinucleotide repeat at peak summits.

Supplementary Figure 7

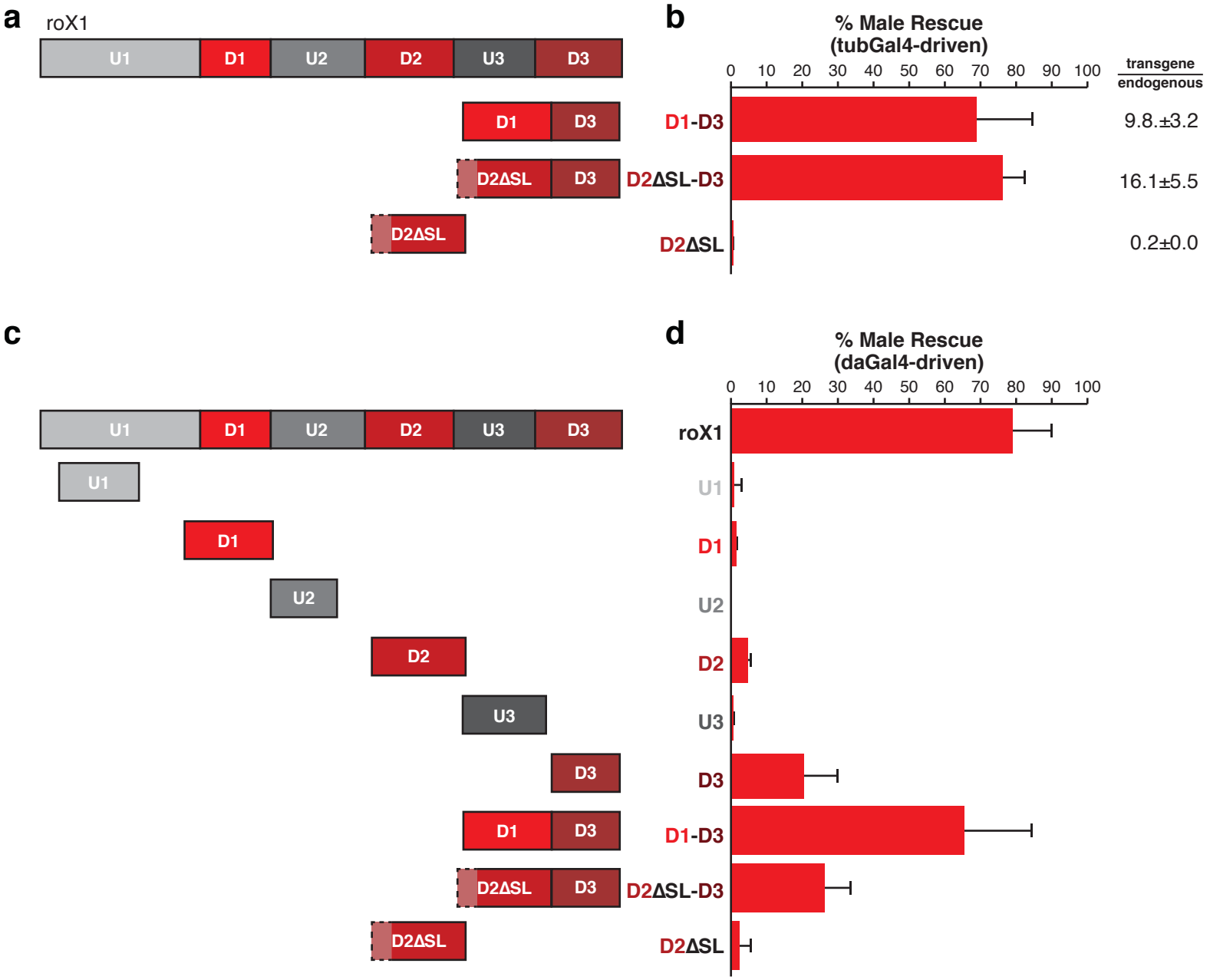

**Supplementary Figure 7**

Additional roX1 transgene mutant rescues.

(**a,c**) Transgene designs. Transgenic constructs of full-length roX1, individual domains, two-domain fusions, and a truncated D2 missing a predicted stem-loop (D2ΔSL) were cloned, chromosomally integrated, and expressed under the tubulin-GAL4 promoter (**a**) or the daughterless-GAL4 promoter (**c**) in *roX*-null flies (see also **Fig. 6**).

(**b,d**) Rescue of male lethality by roX1 transgenes. Transgenic males surviving to adulthood were counted and normalized to females for tubulin-GAL4 transgenes (**b**) or the daughterless-GAL4 transgenes (**d**). Average of three independent crosses +s.d. shown (on average, *n*=800). (**b**) roX transgene expression was quantified and normalized to endogenous roX1 expression in wild-type males, represented as relative fold (transgene/endogenous) ±s.d.